molecules

MDPI

Article

Two New Apotirucallane-Type Triterpenoids from the Pericarp of *Toona sinensis* and Their Ability to Reduce Oxidative Stress in Rat Glomerular Mesangial Cells Cultured under High-Glucose Conditions

Di Liu, Rong-shen Wang, Lu-lu Xuan, Xiao-hong Wang * and Wan-zhong Li *

School of Pharmacy, Weifang Medical University, Weifang 261053, Shandong Province, China; ld0928928@163.com (D.L.); wangrs199012@126.com (R.-s.W.); xuanll1995@163.com (L.-l.X.)

* Correspondence: wangxh@wfmc.edu.cn (X.-h.W.); liwz@wfmc.edu.cn (W.-z.L.); Tel: +86-536-8462493 (X.-h.W.); +86-536-8462490(W.-z.L.)

Received: 21 January 2020; Accepted: 12 February 2020; Published: 12 February 2020

Abstract: Hyperglycemia is a strong risk factor for chronic complications of diabetes. Hyperglycemic conditions foster not only the production of reactive oxygen species (ROS), but also the consumption of antioxidants, leading to oxidative stress and promoting the occurrence and progression of complications. During our continuous search for antioxidant constituents from the pericarp of *Toona sinensis* (A. Juss.) Roem, we isolated two previously unreported apotirucallane-type triterpenoids, toonasinensin A (**1**) and toonasinensin B (**2**), together with five known apotirucallane-type triterpenoids (**3**–**7**) and two known cycloartane-type triterpenoids (**8**–**9**) from the pericarp. Compounds **8**–**9** were obtained from *T. sinensis* for the first time. Their structures were characterized based on interpretation of spectroscopic data (1D, 2D NMR, high-resolution electrospray ionization mass spectra, HR-ESI-MS) and comparison to previous reports. Compounds (**2**, **4**, **6**, **7**, and **9**) were able to inhibit proliferation against rat glomerular mesangial cells (GMCs) cultured under high-glucose conditions within a concentration of 80 μM. Compounds (**2**, **6**, and **7**) were tested for antioxidant activity attributable to superoxide dismutase (SOD), malondialdehyde (MDA), and ROS in vitro, and the results showed that compounds (**2**, **6**, and **7**) could significantly increase the levels of SOD and reduce the levels of MDA and ROS. The current studies showed that apotirucallane-type triterpenoids (**2**, **6**, and **7**) might have the antioxidant effects against diabetic nephropathy.

Keywords: *Toona sinensis* (A. Juss.) Roem; apotirucallane-type triterpenoid; cycloartane-type triterpenoid; rat glomerular mesangial cells; oxidative stress

1. Introduction

Diabetic nephropathy (DN) is one of the most common complications of diabetes, and the occurrence and development of oxidative stress play an important role [1,2]. High-glucose levels can increase the accumulation of reactive oxygen species (ROS) by promoting the generation of ROS and inhibiting the activity of antioxidant enzymes in cells. Excessive oxidative stress could lead to inflammation, fibrosis, the cell apoptosis, and cell damage and death, which are also considered as an important pathological change in DN [3]. There is an urgent need to identify previously unreported antioxidant constituents.

Toona sinensis (A. Juss.) Roem is traditional Chinese medicine belonging to the genus *Toona* and the family Meliaceae, which is widely distributed across Asia [4,5]. *T. sinensis* is rich in triterpenoids, phenols, alkaloids, saponins, sterols, coumarin, and anthraquinone [6–9]. *T. sinensis* had been shown to possess a variety of pharmacological activities, including antioxidant [10], anti-inflammatory [11], bactericidal [12], analgesic [13], antiviral [14], and regulating blood sugar level [14,15].

No study has yet reported the extraction and separation of chemical components in the pericarp of *T. sinensis*, which is often discarded as waste. In the search for potential antioxidant constituents, we performed a chemical investigation and bioactive evaluation of compounds from the pericarp of *T. sinensis*. We described the isolation and structures of two previously unreported apotirucallane-type triterpenoids, toonasinensin A (**1**) and toonasinensin B (**2**), and those of five known apotirucallane-type triterpenoids (**3–7**) and two known cycloartane-type triterpenoids (**8–9**) (Figure 1). The reducing oxidative stress activities of compounds **1–9** were evaluated in rat glomerular mesangial cells (GMCs) cultured under high-glucose conditions.

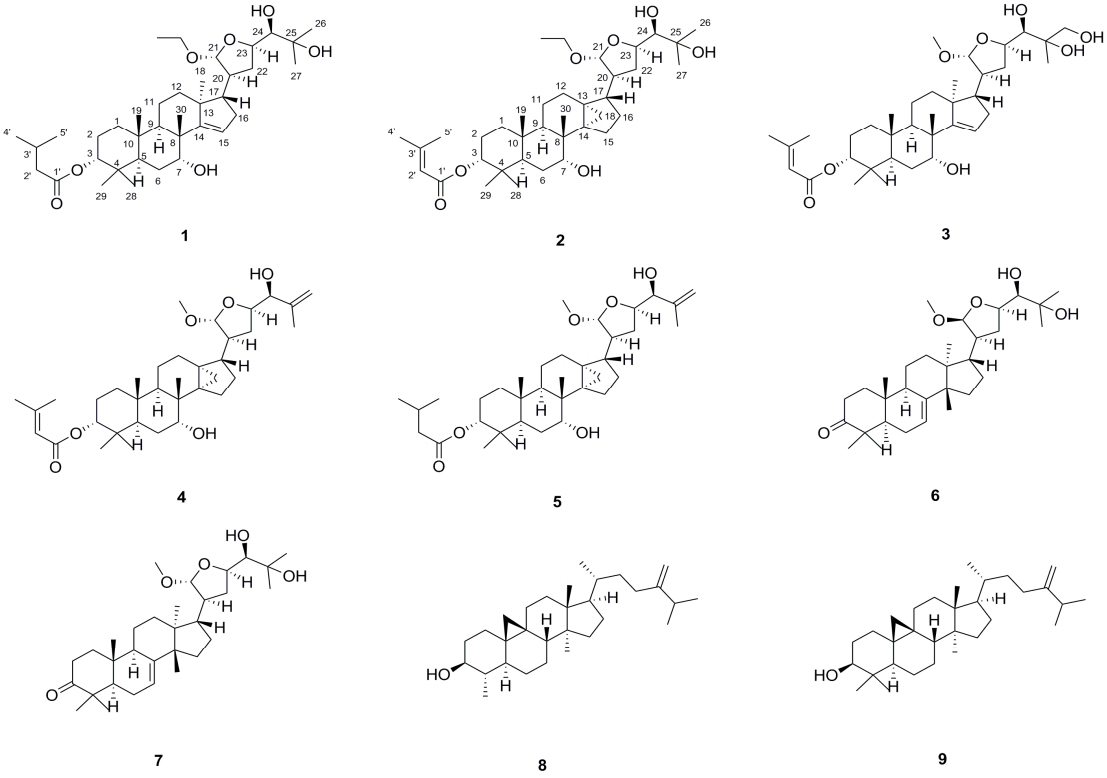

Figure 1. Structures of compounds **1–9** from the pericarp of *T. sinensis*.

2. Results and Discussion

Compound **1** was obtained as a white amorphous powder. Its molecular formula was assigned as $C_{37}H_{62}O_7$ by high-resolution electrospray ionization mass spectra (HR-ESI-MS) (Figure S7) at *m*/*z* 617.44177 $[M–H]^-$ (calculated. 617.44228). The ^{1}H-NMR spectrum (Figure S1) exhibited an olefinic proton at δ_H 5.44 (1H, broad singlet (br s), H-15); five hydroxy methine protons at δ_H 4.92 (1H, d, *J* = 3.3 Hz, H-21), 4.65 (1H, m, H-3), 4.27 (1H, m, H-23), 3.94 (1H, br s, H-7), and 3.24 (1H, m, H-24); one hydroxy methylene group at δ_H 3.76 (1H, m, 21-O*CH*$_2$CH$_3$a), 3.46 (1H, m, 21-O*CH*$_2$CH$_3$b); and 10 methyl groups at δ_H 1.26 (3H, s, H-26), 1.20 (6H, s, H-27, 21-OCH$_2$*CH*$_3$), 1.11 (3H, s, H-18), 1.09 (3H, s, H-29), 0.98 (3H, s, H-19), 0.96 (6H, s, H-4′, 5′), 0.93 (3H, s, H-30), and 0.86 (3H, s, H-28). The ^{13}C-NMR spectrum (Figure S2) displayed one carbonyl carbon at δ_C 174.6 (C-1′); one double bond group at δ_C 162.7 (C-14), 120.3 (C-15); five hydroxy methine signals at δ_C 109.7 (C-21), 79.7 (C-3), 78.4 (C-24), 77.1 (C-23), and 73.7 (C-7); one hydroxy methylene signal at δ_C 64.8 (21-O*CH*$_2$CH$_3$); and 10 methyls at δ_C 28.6 (C-29), 27.5 (C-28), 27.0 (C-26), 25.3 (C-27), 22.3 (C-30), 19.6 (C-18), and 15.8 (C-19, 21-OCH$_2$*CH*$_3$).

All the above NMR data suggested that compound **1** possess an apotirucallane-type triterpenoid skeleton [7,16,17]. Analysis of the HMBC spectrum (Figure 2) demonstrated the isovaleryl ester group was located in C-3 by the cross-signal from H-3 (δ_H 4.65) to C1′ (δ_C 174.6), H-4′ (δ_H 0.96) to C-3′ (δ_C 44.7) and C-2′ (δ_C 25.3), H-5′ (δ_H 0.96) to C-3′ (δ_C 44.7) and C-2′ (δ_C 25.3), and H-29 (δ_H 1.09) and H-28 (δ_H 0.86) to C-3 (δ_C 79.7). The HMBC correlation (Figure 2) between H-30 (δ_H 0.93) and C-7 (δ_C 73.7) indicated that the hydroxyl group was located at C-7 position. The HMBC correlations (Figure 2) between H-15 (δ_H 5.44) and C-16 (δ_C 35.9), C-17 (δ_C 59.3) revealed the presence of a double bond between C-14 and C-15. All the data above indicated that the basic structure of **1** was similar to those of dictamnin B [17], except that the presence of 21-OCH_3 was replaced by 21-OCH_2CH_3 and 26-CH_2OH was replaced by 26-CH_3 in **1**. This was additionally confirmed by the key HMBC correlations (Figure 2) from H-21 (δ_H 4.92) to 21-O*C*H_2CH_3 (δ_C 64.8), 21-OCH_2*C*H_3 (δ_H 1.20) to 21-O*C*H_2CH_3 (δ_C 64.8). The HMBC correlations (Figure 2) between the methyl proton signal H-26 (δ_H 1.26) and H-27 (δ_H 1.20) correlated with C-24 (δ_C 78.4), C-25 (δ_C 73.9), which indicated that the two methyl groups should be located at C-26 and C-27 position, respectively. The NOESY correlations (Figure 2) between H-3/CH_3-29, H-5/CH_3-28, H-7/CH_3-30, H-9/CH_3-18, H-17/CH_3-30, CH_3-19/CH_3-29, and CH_3-19/CH_3-30 showed that isovaleryl ester group, H-5, OH-7, H-9, CH_3-18, and CH_3-28, was α-oriented, whereas H-17, CH_3-19, CH_3-29, and CH_3-30 were β-oriented. Furthermore, The NOESY correlations (Figure 2) were also observed between H-17/H-21, H-21/H-22β, H-22α/H-23, H-20/H-23, and H-23/H-24, which were possible only when **1** possessed 20*S*, 21*R*, 23*R*, and 24*R* configuration. Therefore, compound **1** was identified as toonasinensin A.

Compound **2** was obtained as a white amorphous powder. Its molecular formula was determined as $C_{37}H_{60}O_7$ by the positive HR-ESI-MS (Figure S14) at *m*/*z* 615.42554 $[M–H]^-$ (calculated. 615.42663). The ^{1}H-NMR spectrum (Figure S8) displayed an olefinic proton at δ_H 5.77 (1H, s, H-2′); five hydroxy methine proton at δ_H 4.96 (1H, m, H-21), 4.62 (1H, m, H-3), 4.24 (1H, m, H-23), 3.72 (1H, br s, H-7), and 3.22 (1H, m, H-24); one hydroxy methylene proton at δ_H 3.68 (1H, m, 21-O*C*$H_2$$CH_3$a), 3.40 (1H, m, 21-O*C*$H_2$$CH_3$b); and nine methyl groups at δ_H 2.17 (3H, s, H-5′), 1.92 (3H, s, H-4′), 1.25 (3H, s, H-27), 1.20 (3H, s, H-26), 1.05 (3H, s, H-30), 0.95 (3H, overlap, H-19), 0.92 (3H, overlap, 21-OCH_2*C*H_3), 0.91 (3H, overlap, H-29), and 0.83 (3H, s, H-28). The ^{13}C-NMR spectrum (Figure S9) showed one carbonyl group at δ_C 166.7 (C-1′); one olefinic carbon group at δ_C 156.2 (C-3′) and 116.2 (C-2′); seven oxygenated carbons at δ_C 109.1 (C-21), 77.4 (C-3), 77.1 (C-24), 75.9 (C-23), 74.0 (C-7), 72.5 (C-25), and 67.7 (21-O*C*$H_2$$CH_3$); and nine methyl groups at δ_C 26.8 (C-28), 26.0 (C-4′), 25.9 (C-27), 24.1 (C-26), 20.9 (C-29), 19.1 (C-5′), 18.8 (C-30), 14.7 (C-19), and 12.8 (21-OCH_2*C*H_3). All the data above indicated that the basic structure of **2** was also an apotirucallane-type triterpenoid, and the NMR data were similar to those of apotirucallane triterpenoid compound **1** from the literature [16], except that the presence of 21-OCH_3 was replaced by 21-OCH_2CH_3 in **2**, which was confirmed by the key HMBC correlations (Figure 2) from H-21 (δ_H 4.96) to 21-O*C*$H_2$$CH_3$ (δ_C 67.7) and 21-OCH_2*C*H_3 (δ_C 12.8). The configuration of compound **2** was determined on the NOESY correlations (Figure 2) between H-3/CH_3-29, H-5/CH_3-28, H-7/CH_3-30, H-17/CH_3-30, H-17/H-21, H-21/H-22β, H-22α/H-23, and H-23/H-24. Consequently, the structure of compound **2** was named as toonasinensin B.

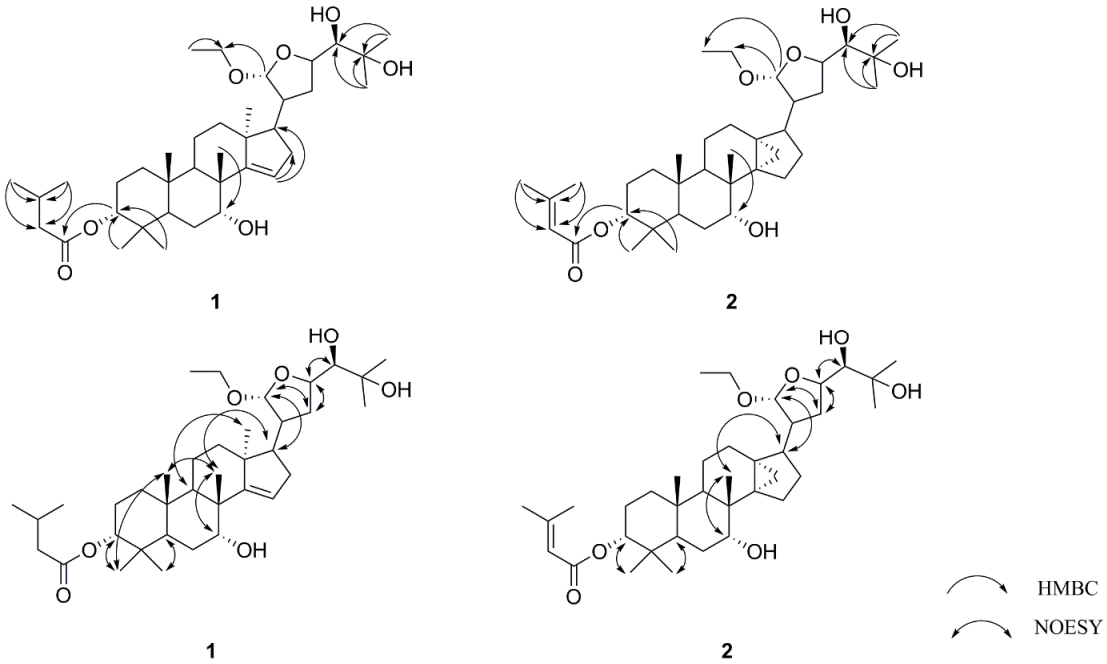

Figure 2. Key HMBC and NOESY correlations of compounds **1–2.**

The other known triterpenoids were identified as toonasinensin C (**3**) [7], toonasinensin D (**4**) [16], toonasinensin E (**5**) [18,19], 21β-*O*-methylmelianodiol (**6**) [20,21], 21α-*O*-methylmelianodiol (**7**) [22], cycloeucalenol (**8**) [23], and 24-methylenecycloartanol (**9**) [24,25].

All compounds (**1–9**) were assessed for their cytotoxicity against GMCs. Compounds **2**, **4**, **6**, **7**, and **9** showed no cytotoxicity against GMCs at 80 μM compared with the normal group (NG) (Figure S15). The proliferation of GMCs is the main pathologic feature of DN, and a variety of stimuli were found to be associated with that proliferation, including high-glucose [26–29]. We investigated the effects of compounds (**2**, **4**, **6**, **7**, and **9**) on GMCs proliferation. As shown in Figure 3, GMCs proliferation became significantly greater than in the NG upon exposure to the high-glucose group (HG). However, treatment with compounds (**2**, **4**, **6**, **7**, and **9**) significantly inhibited high-glucose induced GMCs proliferation.

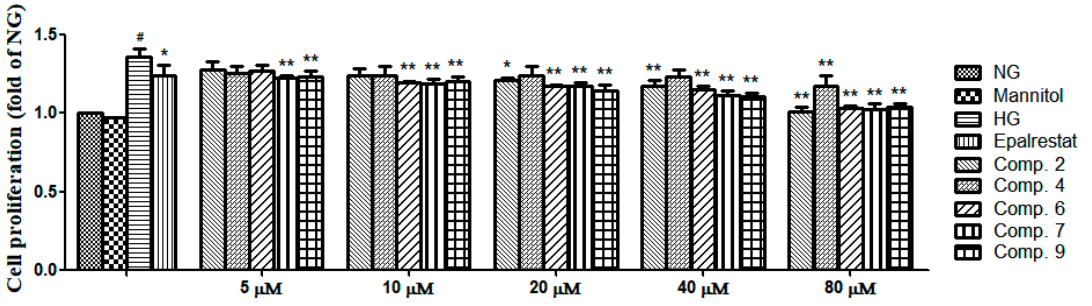

Figure 3. The rat glomerular mesangial cells (GMCs) were pretreated with various concentrations of compounds **2**, **4**, **6**, **7**, and **9** (5, 10, 20, 40, and 80 μM) and incubated for 48 h. GMCs proliferation was determined using the 3-(4, 5-dimethyl-2-thiazolyl)-2, 5-diphenyl-2-H-tetrazolium bromide (MTT) assay. Values are expressed as mean ± SD of three independent experiments, with $^{\#}p < 0.01$ relative to the 5.6 mM glucose (normal group, NG), and $^{**}p < 0.01$, $^{*}p < 0.05$ relative to the 25 mM high glucose (high-glucose group, HG).

Oxidative stress caused by high glucose is a major process in the progression of DN. In order to determine the effect of high glucose on oxidative stress of GMCs, we determined the levels of

superoxide dismutase (SOD), malondialdehyde (MDA), and ROS. The GMCs were treated at concentrations of 10, 30, and 50 μM. The results showed that compounds **2**, **6**, and **7** could render the level of SOD higher than in the HG (Figure 4). Compounds **2**, **6**, and **7** could render the levels of MDA and ROS lower than in the HG (Figures 5 and 6). These results indicated that they could significantly reduce oxidative stress of GMCs. A preliminary structure-activity relationship indicated that apotirucallane-type triterpenoids (**2**, **6**, and **7**) showed significant antioxidant effects with respect to DN; nevertheless cycloartane-type triterpenoids (**8**–**9**) had no antioxidant activities. Even more interesting was that compounds **6** and **7** possessed similar activities, perhaps because the stereochemistry of C-21 could not affect the strength of antioxidant activities. In this way, apotirucallane-type triterpenoids have the potential for further development and research.

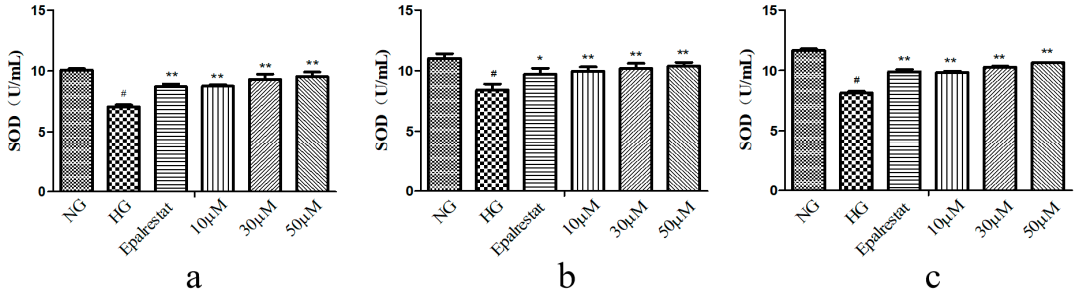

Figure 4. Compounds **2 (a)**, **6 (b)**, and **7 (c)** increased the levels of superoxide dismutase (SOD) induced by high glucose in GMCs. GMCs were incubated with or without compounds **2**, **6**, and **7** (10, 30, and 50 μM) in the 5.6 mM glucose (normal group, NG) or 25 mM high glucose (high-glucose group, HG) for 48 h. $^{\#}p < 0.01$ compared with the NG, and $^{**}p < 0.01$, $^{*}p < 0.05$ relative to the HG.

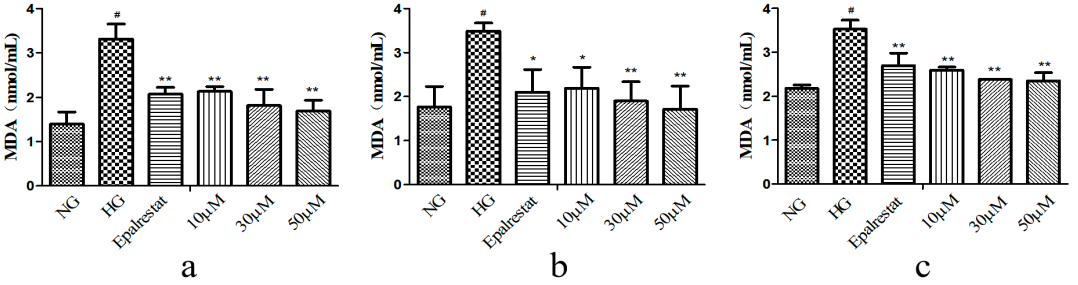

Figure 5. Compounds **2 (a)**, **6 (b)**, and **7 (c)** inhibited the marker of oxidative stress malondialdehyde (MDA) by high- glucose in GMCs. GMCs were incubated with or without compounds **2**, **6**, and **7** (10, 30, and 50 μM) in the 5.6 mM glucose (normal group, NG) or 25 mM high glucose (high-glucose group, HG) for 48 h. $^{\#}p < 0.01$ relative to the NG, and $^{**}p < 0.01$, $^{*}p < 0.05$ compared with the HG.

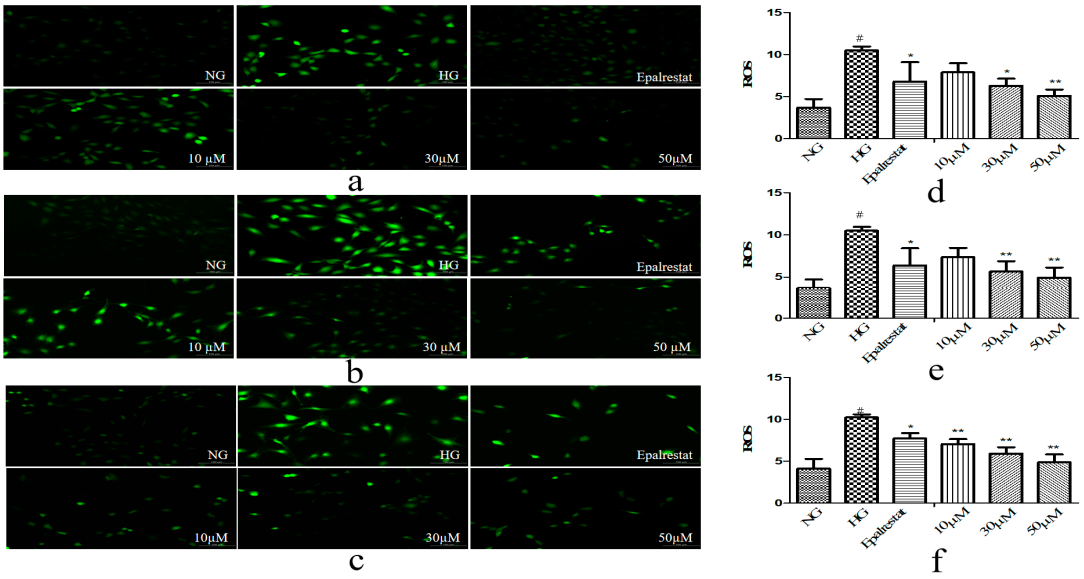

Figure 6. Compounds **2 (a,d)**, **6 (b,e)**, and **7 (c,f)** inhibited the marker of oxidative stress reactive oxygen species (ROS) induced by high glucose in GMCs. GMCs were incubated with or without compounds **2**, **6**, and **7** (10, 30, and 50 μM) under the 5.6 mM glucose (normal group, NG) or 25 mM high glucose (high-glucose group, HG) for 48 h. $^{\#}p < 0.01$ relative to the NG, and $^{**}p < 0.01$, $^{*}p < 0.05$ relative to the HG.

3. Materials and Methods

3.1. General Experimental Procedures

High-resolution electrospray ionization mass spectra (HR-ESI-MS) were obtained using a Bruker microsoft time-of-flight QII mass spectrometer (Bruker Daltonics, Fremont, CA, USA). The NMR spectra were recorded using Bruker AV 500MHz spectrometer (Bruker, Fällanden, Switzerland). Optical rotation was measured using a Rudolph Autopol I automatic polarimeter (Rudolph Research Analytical, Hackettstown, NJ, USA). Column chromatography was performed using silica gel (200–300 mesh, Branch of Qingdao Haiyang Chemical Co., Ltd., Qingdao, China) and Sephadex LH-20 (Shanghai Yuanye Biological Technology Co., Ltd., Shanghai, China). Lichroprep RP-18 gel (40–60 μm) was purchased from Merck KGaA (Darmstadt, Germany). Thin layer chromatography (TLC) was performed with precoated silica gel GF 254 glass plates (100 × 200 mm, Branch of Qingdao Haiyang Chemical Co., Ltd.). All other chemicals and solvents were analytical grade and used without further purification.

3.2. Plant Material

The pericarp of *T. sinensis* was collected by the Jinan Shengke Technology Company of China and identified by Prof. Chongmei Xu. A voucher specimen (voucher number: WF-YXY-1712) has been deposited at the Pharmacognosy Laboratory of the School of Pharmacy, Weifang Medical University.

3.3. Extraction and Isolation

Dried pericarp of *T. sinensis* (20 kg) was extracted three times with 95% EtOH (100 L × 3 times) and heated for 10 h. The combined extracts were concentrated under a vacuum to obtain a crude extract (854 g). The crude extract was suspended in H_2O (3 L) and partitioned sequentially with CH_2Cl_2, EtOAc, and *n*-BuOH (3 L × 3 times in each case). The CH_2Cl_2 extract (147 g) was rested after evaporations. The CH_2Cl_2 extract was dissolved in the mixed solvent of CH_2Cl_2-MeOH, and silica gel (185 g) was added to conduct dry sample mixing before further fractionation. The CH_2Cl_2 extract

(147 g) was purified by silica gel column chromatography and eluted with a gradient of petroleum ether:EtOAc (30:1, 10:1, 5:1, 2:1, *v*/*v*) and CH_2Cl_2:MeOH (20:1, 5:1, *v*/*v*) to generate 6 fractions (Fr. A-F). Fractions that flowed out of the column chromatography were combined based on their TLC patterns in the whole separation experiment. Fr. A (20 g) was separated chromatographically using octade-cylsilyl (ODS) and eluted with MeOH-H_2O (from 40% to 100%) to produce 12 subfractions (Fr. A1-A12). Fr. A7 (4.6 g) was separated using a gradient of petroleum ether:EtOAc (from 80:1 to 40:1) to produce 5 fractions (Fr. A71-A75). Fr. A74 (1.4 g) was separated using Sephadex LH-20 to give compound **3** (54.5 mg). Fr. B (30 g) was separated chromatographically using ODS and eluted with MeOH-H_2O (from 40% to 100%) to produce 9 subfractions (Fr. B1-B9). Fr. B8 (9.1 g) was separated using silica gel with a gradient of petroleum ether:EtOAc (from 45:1 to 30:1) to produce 4 fractions (Fr. B81-B84). Fr. B83 was separated using silica gel with a gradient of petroleum ether:EtOAc (from 80:1 to 60:1) to give compound **9** (21.3 mg). Fr. B84 was separated using silica gel with a gradient of petroleum ether:EtOAc (from 70:1 to 50:1) to produce 10 fractions (Fr. B841-B8410). Fr. B848 was separated using ODS and eluted with MeOH-H_2O (from 88% to 100%) to give compound **8** (142.2 mg). Fr. C (20 g) was separated chromatographically using ODS and eluted with MeOH-H_2O (from 30% to 100%) to produce 10 subfractions (Fr. C1-C10). Fr. C9 (7.2 g) was separated using silica gel with a gradient of petroleum ether:EtOAc (from 10:1 to 5:1) to produce 4 fractions (Fr. C91-C94). Fr. C92 (1.2 g) was separated using silica gel with a gradient of petroleum ether:EtOAc (from 9:1 to 7:1) to give compound **5** (17.9 mg). Fr. C93 (1.2 g) was separated using silica gel with a gradient of petroleum ether:EtOAc (from 9:1 to 7:1) to produce 4 fractions (Fr. C931-C934). Fr. C931 (0.4 g) was separated using ODS and eluted with MeOH-H_2O (from 75% to 85%) to give compound **6** (17.2 mg). Fr. C932 (0.35 g) was separated using ODS and eluted with MeOH-H_2O (from 75% to 80%) to give compound **7** (12.9 mg). Fr. D (20 g) was separated using ODS and eluted with MeOH-H_2O (from 30% to 90%) to produce 13 subfractions (Fr. D1-D13). Fr. D9 (5.4 g) was separated using silica gel with a gradient of petroleum ether:EtOAc (from 7:1 to 4.5:1) to produce 5 fractions (Fr. D91-D95). Fr. D94 (2.6 g) was isolated using Sephadex LH-20 to obtain compound **1** (12 mg). Fr. D10 (8 g) was separated using silica gel with a gradient of petroleum ether:EtOAc (from 6:1 to 3:1) to produce 5 fractions (Fr. D101-D105). Fr. D101 (1.5 g) was isolated using Sephadex LH-20 to obtain compound **4** (17.9 mg). Fr. D105 was isolated using ODS and eluted with MeOH-H_2O (75%) to give compound **2** (6 mg) (Figure S16).

3.3.1. Toonasinensin A (1)

White amorphous powder; $C_{37}H_{62}O_7$; $[\alpha]_D^{24}$ - 20.64 (*c* 0.17, MeOH); HR-ESI-MS *m*/*z* 617.44177 [M –H]$^-$ (calcd. 617.44228); ^{1}H-NMR (methanol-d_4, 500 MHz) and ^{13}C-NMR data (methanol-d_4, 125 MHz), which were unambiguously assigned by distortionless enhancement by polarization transfer (DEPT) 135, HMQC, HMBC, and NOESY experiments (Figures S3–S6) (see Table 1).

3.3.2. Toonasinensin B (2)

White amorphous powder; $C_{37}H_{60}O_7$; $[\alpha]_D^{24}$ - 14.73 (*c* 0.08, MeOH); HR-ESI-MS *m*/*z* 615.42554 [M –H]$^-$ (calcd. 615.42663); ^{1}H-NMR (methanol-d_4, 500 MHz) and ^{13}C-NMR data (methanol-d_4, 125 MHz), which were unambiguously assigned by DEPT 135, HMQC, HMBC, and NOESY experiments (Figures S10–S13) (see Table 1).

Table 1. The ^{1}H- and ^{13}C-NMR data (500 and 125 MHz) of compounds **1** and **2** (δ in ppm) in methanol-d_4.

Pos.	1		2	
	δ_C	δ_H (*J* in Hz)	δ_C	δ_H (*J* in Hz)
1	34.6	1.40 m, 1.27 m	33.6	1.38 m, 1.21 m
2	23.8	1.95 m, 1.63 m	22.5	1.97 m, 1.54 m
3	79.7	4.65 m	77.4	4.62 m
4	37.3	-	36.3	-

5	43.0	2.07 m	41.2	2.01 m
6	23.8	2.03 m, 1.54 m	24.5	1.68 m, 1.57 m
7	73.7	3.94 br s	74.0	3.72 br s
8	45.2	-	39.1	-
9	43.2	2.06 m	44.1	1.39 m
10	38.8	-	37.2	-
11	17.5	1.69 m, 1.54 m	16.1	1.32 m
12	34.4	1.87 m, 1.49 m	25.4	1.87 m
13	48.1	-	28.4	-
14	162.7	-	36.1	-
15	120.3	5.44 br s	25.6	1.92 m, 1.55 m
16	35.9	2.16 m	25.7	1.67 m
17	59.3	1.71 m	48.6	1.99 m
18	19.6	1.11 s	13.5	0.72 m, 0.51 m
19	15.8	0.98 s	14.7	0.95 overlap
20	47.5	2.33 m	49.1	2.06 m
21	109.7	4.92 d (3.3)	109.1	4.96 m
22	36.1	1.94 m, 1.65 m	31.7	1.59 m, 1.51 m
23	77.1	4.27 m	75.9	4.24 m
24	78.4	3.24 m	77.1	3.22 m
25	73.9	-	72.5	-
26	27.0	1.26 s	24.1	1.20 s
27	25.3	1.20 s	25.9	1.25 s
28	27.5	0.86 s	26.8	0.83 s
29	28.6	1.09 s	20.9	0.91 overlap
30	22.3	0.93 s	18.8	1.05 s
1′	174.6	-	166.7	-
2′	25.3	1.19 m	116.2	5.77 s
3′	44.7	2.23 m	156.2	-
4′	22.8	0.96 s	26.0	1.92 s
5′	22.8	0.96 s	19.1	2.17 s
21-O*CH*$_2$CH$_3$	64.8	3.76 m, 3.46 m	67.7	3.68 m, 3.40 m
21-OCH$_2$*CH*$_3$	15.8	1.20 s	12.8	0.92 overlap

3.4. Cytotoxicity Assay

Cytotoxic activity against GMCs (Keygen Biotechnology, Nanjing, China) was measured using the 3-(4, 5-dimethylthiazol-2-yl)-2, 5-diphenyl tetrazolium (MTT) method. GMCs (5×10^3 cells/well) in Dulbecco's Modified Eagle Medium (DMEM) with 10% fetal bovine serum (FBS) were plated into 96-well plates. Then GMCs were cultured with 5.6 mM glucose (normal group, NG) or NG medium in the presence of compounds (**1**–**9**) (80 μM) for 48 h, followed by the addition of 100 μL of the MTT solution (0.5 mg/mL) to each well and further incubation for 4 h. The medium was removed and the dark blue crystals in each well were dissolved in 100 μL dimethyl sulfoxide (DMSO). The absorbance of the wells was measured with a microplate reader at test and reference wavelength of 490 nm.

3.5. Cell Proliferation Assay

GMCs were plated into 96-well plates. Then GMCs were divided into NG, NG medium in the presence of mannitol (25 mM), 25 mM high glucose (high-glucose group, HG), HG medium in the presence of epalrestat (10 μM), and HG medium in the presence of compounds (**2**, **4**, **6**, **7**, and **9**) (5, 10, 20, 40, and 80 μM). Cell proliferation was measured using the MTT assay. Mannitol was used as osmotic pressure group and epalrestat was used as positive control.

3.6. In Vitro Antioxidant Activity of SOD, MDA, and ROS

3.6.1. SOD

Superoxide dismutase is an important antioxidant enzyme defense in all organisms [30]. SOD levels were detected by Nanjing Jiancheng Bioengineering Institute assay kit. GMCs were cultured in a 6-well plate at 3×10^5 cells/well and exposed to the compounds (10, 30, and 50 μM) for 48 h. Absorbance was recorded at 450 nm using microplate reader. SOD activity is expressed as (U/mL), where each unit represents the amount of enzyme. The disproportionation of 50% superoxide radicals needs to be revealed.

3.6.2. MDA

MDA is an indicator of lipid peroxidation. MDA was detected by Nanjing Jiancheng Bioengineering Institute assay kit [31,32]. GMCs were cultured in a 6-well plate at 3×10^5 cells/mL and exposed to the compounds (10, 30, and 50 μM) for 48 h. Absorbance was recorded at 532 nm using microplate reader.

3.6.3. ROS

Medium and high concentrations of ROS induce cell apoptosis and even necrosis through cell oxidative stress reaction [33,34]. GMCs were cultured in a 96-well plate at 5×10^3 cells/well and exposed to the compounds (10, 30, and 50 μM) for 48 h. The cells' supernatant was discarded and determined ROS by reactive oxygen species assay kit (Beijing Solarbio Science and Technology Co., Ltd.). Measured fluorescence intensity with fluorescence microplate reader at excitation and emission wavelengths of 488 and 525 nm.

3.7. Statistical Analysis

Statistical differences between two groups were analyzed by the T-test and differences between multiple groups of data were analyzed by one-way ANOVA with the prism software (GraphPad, San Diego, CA), and the data were expressed as the mean ± SD of three independent experiments. A *P* value of less than 0.05 was considered statistically significant.

4. Conclusions

Nine compounds were isolated from the pericarp of *T. s*inensis, including two previously unreported apotirucallane-type triterpenoids, toonasinensin A (**1**) and toonasinensin B (**2**); five known apotirucallane-type triterpenoids (**3**–**7**); and two known cycloartane-type triterpenoids (**8**–**9**). Compounds **2**, **4**, **6**, **7**, and **9** were found to significantly inhibit high-glucose induced GMCs proliferation. Compounds **2**, **6**, and **7** were able to significantly increase the vitality of SOD and reduce the levels of MDA and ROS. In summary, compounds **2**, **6**, and **7** were able to prevent DN by reducing oxidative stress, indicating that *T. s*inensis is worthy of further exploration to find more novel constituents with potential bioactivity.

Supplementary Materials: The following are available online: Figures S1–S14: HR-ESI-MS and NMR spectra of compounds **1**–**2**; Figure S15: Cytotoxicity assay of compounds **1**–**9** in GMCs.

Author Contributions: This study was conceived and designed by W.-z.L. W.z.L. contributed reagents/materials/analysis tools. The experiments were conducted by D.L., R.-s.W., L.-l.X., and X.-h.W. R.-s.W. analyzed the data. The manuscript was drafted by D.L. X.-h.W. and W.-z.L. finalized the manuscript. All authors read and approved the content of the manuscript.

Funding: This research was funded by the National Nature Science Foundation of China (81274049), Natural Science Foundation of Shandong Province (ZR2018MH040), Shandong Science and Technology Research Project of Traditional Chinese Medicine (2015227), and Staring Foundation for Doctorate Research of Weifang medical university (2017BSQD50).

Acknowledgments: We thank LetPub for its linguistic assistance during the preparation of this manuscript.

Conflicts of Interest: The authors declare no conflict of interest.

References

1. Dong, A.; Tan, X.Y.; Kong, Q.; Zhang, M.Z. Protective Effect and Mechanism of Schisandra Chinensis Ethanol Extract on Oxidative Stress in Diabetic Nephropathy Mice. *Chin. Tradit. Herb. Drugs* **2019**, *50*, 6038–6044.
2. Li, S.Y.; Li, W.J.; Wu, R.Y.; Sargsyan, D.; Raskin, I.; Kong, A.N. Epigenome and transcriptome study of moringa isothiocyanate in mouse kidney mesangial cells induced by high glucose, a potential model for diabetic-induced nephropathy. *AAPS J.* **2019**, *22*, 8.
3. Wang, Z.Q.; Li, Y.; Wang, Y.; Zhao, K.X.; Chi, Y.Q.; Wang, B.X. Pyrroloquinoline quinine protects HK-2 cells against high glucose-induced oxidative stress and apoptosis through Sirt3 and PI3K/Akt/FoxO3a signaling pathway. *Biochem. Biophys. Res. Commun.* **2019**, *508*, 398–404.
4. Yang, H.L.; Chen, S.C.; Lin, K.Y.; Wang, M.T.; Chen, Y.C.; Huang, H.C.; Cho, H.J.; Wang, L.; Kumar, K.J.; Hesu, Y.C. Antioxidant activities of aqueous leaf extracts of *Toona sinensis* on free radical-induced endothelial cell damage. *J. Ethnopharmacology* **2011**, *137*, 669–680.
5. Chen, Y.C.; Chen, H.J.; Huang, B.M.; Chen, Y.C.; Chang, C.F. Polyphenol-rich extracts from *Toona sinensis* bark and fruit ameliorate free fatty acid-induced lipogenesis through AMPK and LC3 pathways. *J. Clin. Med.* **2019**, *8*. 1664-1679.
6. Dong, X.J.; Zhu, Y.F.; Bao, G.H.; Hu, F.L.; Qin, G.W. New limonoids and a dihydrobenzofuran norlignan from the roots of *Toona sinensis*. *Molecules* **2013**, *18*, 2840–2850.
7. Mitsui, K.; Saito, H.; Yamamura, R.; Fukaya, H.; Hitotsuyanagi, Y.; Takeya, K. Apotirucallane and tirucallane triterpenoids from *Cedrela sinensis*. *Chem. Pharm. Bull.* **2007**, *55*, 1442–1447.
8. Lee, I.S.; Kim, H.J.; Youn, U.J.; Chen, Q.C.; Kim, J.P.; Ha, D.T.; Ngoc, T.M.; Min, B.S.; Lee, S.M.; Jung, H.J.; et al. Dihydrobenzofuran norlignans from the leaves of *Cedrela sinensis* A. Juss. *Helv. Chim. Acta.* **2010**, *93*, 272–276.
9. Chen, K.W.; Yang, R.Y.; Tsou, S.C.S.; Lo, C.S.C.; Ho, C.T.; Lee, T.C.; Wang, M.F. Analysis of antioxidant activity and antioxidant constituents of Chinese toon. *J. Funct. Foods* **2009**, *1*, 253–259.
10. Li, S.J.; Hu, Y.Q. Antioxidant activity of extracts from *Toona sinensis* leaves. *Anhui Agricultural Sciences* **2007**, *35*, 6807–6808.
11. Xue, L.; Li, C.F. Preliminary pharmacodynamic experiment of total flavonoids from *Toona sinensis* buds. *Shandong Journal of Traditional Chinese Medicine.* **2004**, *23*, 685–686.
12. Chen, Y.K.; Ou, H.P.; Fang, C.L.; Yang, H.H.; Liu, S.B. Determination of antibacterial activity of pericarp of *Toona sinensis* and *Ailanthus altissima* in *vitro*. *Sichuan Animal and Veterinary Sciences* **2011**, *5*, 26–27.
13. Chen, Y.L.; Ruan, Z.P.; Lin, L.S.; Li, C.L. Research progress on chemical constituents and pharmacological effects of *Toona sinensis*. *Journal of Changzhi Medical College* **2008**, *22*, 315–317.
14. Chen, L.; Zhang, J.X.; Wang, B.; Mu, S.Z.; Hao, X.J. Triterpenoids with anti-tobacco mosaic virus activities from *Melia toosendan*. *Fitoterapia* **2014**, *97*, 204–210.
15. Zhang, D.; Jiang, F.L.; Huang, L.; Chen, Y.L.; Shao, L.Q.; Chai, C.B.; Wang, F.X.; Zuo, X.C. Effect of total flavonoids from *Toona sinensis* leaves on blood glucose in diabetic mice. *Northwest Pharmaceutical Journal* **2011**, *4*, 40–41.
16. Mitsui, K.; Maejima, M.; Satio, H.; Fukaya, H.; Hitotsuyanagi, Y.; Takeya, K. Triterpenoids from *Cedrela sinensis*. *Tetrahedron* **2005**, *61*, 10569–10582.
17. Bai, Y.Y.; Jin, X.; Jia, X.H.; Tang, W.T.; Wang, X.J.; Zhao, Y.X. Two new apotirucallane-type isomeric triterpenoids from the root bark of *Dictamnus dasycarpus* with their anti-proliferative activity. *Phytochem. Lett.* **2014**, *10*, 118–122.
18. Lien, T.P.; Kamperdick, C.; Schmidt, J.; Adam, G.; Sung, T.V. Apotirucallane triterpenoids from *Luvunga sarmentosa*. *Phytochemistry* **2002**, *60*, 747–754.
19. Xu, J.Q.; Shen, Q.; Li, J.; Hu, L.H. Dammaranes from *Gynostemma pentaphyllum* and synthesis of their derivatives as inhibitors of protein tyrosine phosphatase 1B. *Bioorg. Med. Chem.* **2010**, *18*, 3934–3939.
20. Zhang, F.; Wang, J.S.; Gu, Y.C.; Kong, L.Y. Cytotoxic and anti-inflammatory triterpenoids from *Toona ciliata*. *J. Nat. Prod.* **2012**, *75*, 538–546.
21. Zhou, F.; Ma, X.H.; Li, Z.J.; Li, W.; Zheng, W.M.; Wang, Z.B.; Zeng, X.M.; Sun, K.H.; Zhang, Y.H. Four new tirucallane triterpenoids from the fruits of Melia azedarach and their cytotoxic activities. *Chem. Biodivers.* **2016**.

22. Wu, W.B.; Zhang, H.; Dong, S.H.; Sheng, L.; Wu, Y.; Li, J.; Yue, J.M. New triterpenoids with protein tyrosine phosphatase 1B inhibition from *Cedrela odorata*. *J. Asian Nat. Prod. Res.* **2014**, *16*, 709–716.
23. Yan, X.T.; Lee, S.H.; Li, W.; Jang, H.D.; Kim, Y.H. Terpenes and sterols from the fruits of *Prunus mume* and their inhibitory effects on osteoclast differentiation by suppressing tartrate-resistant acid phosphatase activity. *Arch. Pharm. Res.* **2015**, *38*, 186–192.
24. Lee, S.Y.; Choi, S.U.; Lee, J.H.; Lee, D.U.; Lee, K.R. A new phenylpropane glycoside from the rhizome of *Sparganium stoloniferum*. *Arch. Pharm. Res.* **2010**, *33*, 515–521.
25. Akihisa, T.; Kimura, Y.; Tamura, T. Cycloartane triterpenes from the fruit peel of *Musa sapientum*. Phytochemistry **1998**, *47*, 1107–1110.
26. Wang, Y.Q.; Fan, C.C.; Chen, B.P.; Shi, J. Resistin-like molecule beta (RELM-β) regulates proliferation of human diabetic nephropathy mesangial cells via mitogen-activated protein kinases (MAPK) signaling pathway. *Med. Sci. Monit.* **2017**, *23*, 3897–3903.
27. Stevenson, F.T.; Shearer, G.C.; Atkinson, D.N. Lipoprotein-stimulated mesangial cell proliferation and gene expression are regulated by lipoprotein lipase. *Kidney Int.* **2001**, *59*, 2062–2068.
28. Yang, X.Q.; Wang, Y.G.; Gao, G.Q. High glucose induces rat mesangial cells proliferation and MCP-1 expression via ROS-mediated activation of NF-κB pathway, which is inhibited by eleutheroside E. *J. Recept. Signal Transduct. Res.* **2016**, *36*, 152–157.
29. Chen, F.; Ma, Y.L.; Sun, Z.Q.; Zhu, X.G. Tangeretin inhibits high glucose-induced extracellular matrix accumulation in human glomerular mesangial cells. *Biomed. Pharmacother.* **2018**, *102*, 1077–1083.
30. C.Azevedo, B.; Roxo, M.; C.Borges, M.; Peixoto, H.; J.Crevelin, E.; W.Bertoni, B.; H.T.Contini, S.; A.Lopes, A.; C.França, S.; M.S.Pereira, A.; et al. Antioxidant activity of an aqueous leaf extract from and its major alkaloids mitraphylline and isomitraphylline in *Caenorhabditis elegans*. *Molecules* **2019**, *24*, 3299.
31. Li, C.N.; Lan, M.; Lv, J.W.; Zhang, Y.; Gao, X.C.; Gao, X.; Dong, L.H.; Luo, G.M.; Zhang, H.; Sun, J.M. Screening of the hepatotoxic components in and their effects on rat liver BRL-3A cells. *Molecules* **2019**, *24*, 3920.
32. Wang, Y.W.; Liang, J.; Luan, G.X.; Zhang, S.D.; Zhuoma, Y.X.; Xie, J.X.; Zhou, W. Quantitative analyses of nine phenolic compounds and their antioxidant activities from thirty-seven varieties of raspberry grown in the qinghai-tibetan plateau region. *Molecules* **2019**, *24*, 3932.
33. Shi, Q.; Dong, X.M.; Zhang, M.; Cheng, Y.H.; Pei, C. Knockdown of ALK7 inhibits high glucose-imacol. *Physiol.* **2020**, *47*, 313–321.
34. Xu, K.; Guo, L.Q.; Bu, H.X.; Wang, H. Daphnetin inhibits high glucose-induced extracellular matrix accumulation, oxidative stress and inflammation in human glomerular mesangial cells. *J. Pharmacol. Sci.* **2019**, *139*, 91–97.

Sample Availability: Samples of the compounds **1–9** are available from the authors.